

TP53, P14^{ARF}, P16^{INK4A} AND H-RAS GENE MOLECULAR ANALYSIS IN INTESTINAL-TYPE ADENOCARCINOMA OF THE NASAL CAVITY AND PARANASAL SINUSES

Federica PERRONE¹, Maria OGGIONNI¹, Sarah BIRINDELLI⁵, Simona SUARDI¹, Silvia TABANO¹, Roberta ROMANO¹, Maria Luisa MOIRAGHI¹, Gabriella BIMBI², Pasquale QUATTRONE¹, Giulio CANTU², Marco A. PIEROTTI³, Lisa LICITRA⁴ and Silvana PILOTTI^{1*}

¹Unit of Experimental Molecular Pathology, Department of Pathology, Istituto Nazionale per lo Studio e la Cura dei Tumori, Milan, Italy

²Department of Head and Neck Surgery, Istituto Nazionale per lo Studio e la Cura dei Tumori, Milan, Italy

³Department of Experimental Oncology, Istituto Nazionale per lo Studio e la Cura dei Tumori, Milan, Italy

⁴Department of Head and Neck, Medical Oncology; Istituto Nazionale per lo Studio e la Cura dei Tumori, Milan, Italy

⁵International Center for Pesticides and Health Risk Prevention, Milan, Italy

Intestinal-type adenocarcinoma (ITAC) of the nasal cavity and paranasal sinuses is an uncommon tumor associated with occupational exposure to dusts of different origin. Few investigations addressed molecular alterations in ITAC mainly focused on TP53, K-ras and H-ras gene mutations. The occurrence of TP53, p14^{ARF} and p16^{INK4a} deregulation and H-ras mutations was investigated in 21 consecutive and untreated ITACs cases, 17 with known professional exposure. No H-ras mutations were found. In patients with known exposure, cumulative evidence of TP53 or p14^{ARF} alterations accounted for 88% and the evidence of p16^{INK4a} alterations for 65%, respectively. TP53 mutations were present in 44% of the ITACs, consisted of G:C→A:T transitions in 86%, and involved the CpG dinucleotides in 50% of the cases. LOH at the locus 17p13 and an uncommon high rate of p53 stabilization were detected in 58% and 59% of the cases, respectively. p14^{ARF} and p16^{INK4a} promoter methylation accounted for 80% and 67% respectively, and LOH at the locus 9p21 occurred in 45% of the cases. Interestingly, all dust-exposed tumors with p16^{INK4a} alterations shared TP53 or p14^{ARF} deregulation. The present results show a close association of this occupational tumor with TP53, p14^{ARF} and p16^{INK4a} gene deregulation. Given the important role that these genes play in cell growth control and apoptosis, the knowledge of ITAC genetic profile may be helpful in selecting more tailored treatments.

© 2003 Wiley-Liss, Inc.

Key words: LOH; TP53 mutation; p14^{ARF}; p16^{INK4a}; methylation; occupational exposure

Intestinal-type adenocarcinoma (ITAC) of the nasal cavity and paranasal sinuses is an uncommon, professional-related tumor characterized by high local aggressiveness and ominous outcome.¹ ITAC encompasses a neoplasm group showing a range of microscopic features spanning from tumors indistinguishable from typical colonic adenocarcinoma to colloid or signet-ring cell carcinoma of the colon.² Surgery is, and still remains, the treatment of choice for this tumor although it has been complemented recently by primary chemotherapy.³

ITAC clearly predominates among males and exhibits an extreme gender distribution likely to be related to an occupational exposure. Several epidemiologic studies pointed out the association of ITAC with professional exposure primarily to wood or leather dust.^{4–8} Dusts of different origin are other potential risk factors for sinonasal adenocarcinomas, including textile,^{9,10} cereal or cement dust.¹¹

The close relationship between professional exposure and ITAC strongly suggests that dusts and chemical elements may be implicated as etiological agents in the tumorigenesis of this tumor. Investigations into the genotoxic action of several substances present in the wood or used by wood- and leather-workers showed the combined genotoxic effects of dusts and chemicals.^{7,8} A variety of chemical carcinogens cause mutations in human tumors by forming covalent adducts that increase the probability of errors

during DNA replication.¹² Some carcinogenic agents may target oncogenes and tumor suppressor genes producing specific types and locations of DNA alterations. These carcinogen-induced mutational spectra are influenced by the specific DNA sequence.¹³ Previous studies showed that methylated CpG dinucleotides may represent preferential targets for mutagens.^{14,15} A strong and selective formation of both adducts and mutations involving CpG islands of the TP53 gene is frequent in human tumors^{16,17} and an association between DNA methylation and exposure to carcinogens, as tobacco¹⁸ and vinyl chloride¹⁹ has been reported recently.

In addition, loss of heterozygosity (LOH) at chromosomal loci encoding the TP53, p14^{ARF} and p16^{INK4a} genes represents a further molecular event related to carcinogenic exposure, as found in tobacco smoke-associated larynx cancer.²⁰ Moreover, TP53 mutations and p16^{INK4a} deletion or hypermethylation correlate with early genetic changes in malignancy development of the Barrett's esophagus^{21,22} and frequently occur as late events in colorectal adenocarcinoma.^{23–25}

Few investigators addressed molecular alterations in ITACs. In the assumption that morphologic resemblance with colorectal cancer might reflect equivalent genetic alterations, Wu *et al.*²⁶ carried out TP53 gene analysis in 12 ITAC with unknown professional exposure showing p53 immunoreactivity and TP53 mutations in 58% and 18% of the cases, respectively. Mutational analysis restricted to *ras* oncogenes was also carried out and evidence of K-ras²⁷ and H-ras²⁸ activation was found in 1 of 12 (8%) and in 5 of 31 (16%) ITACs, respectively.

We investigated the occurrence of TP53, p14^{ARF} and p16^{INK4a} deregulation and H-ras mutations in 21 consecutive untreated ITAC cases, 17 of which with known professional exposure. No H-ras mutations were found. By contrast, in patients with known exposure, the results suggest a close relationship between dust exposure and TP53 and INK4a-ARF alterations, represented by the high percentage of TP53 mutations (44%). In all but 1 case the

Grant sponsor: AIRC/FIRC (Associazione and Fondazione Italiana per la Ricerca sul Cancro).

*Correspondence to: Unit of Experimental Molecular Pathology, Department of Pathology, Istituto Nazionale per lo Studio e la Cura dei Tumori, Via G. Venezian, 1, 20133 Milano, Italy. Fax: +39-2-23902756. E-mail: silvana.pilotti@istitutotumori.mi.it

Received 3 September 2002; Revised 2 December 2002; Accepted 10 January 2003

DOI 10.1002/ijc.11062

mutations were of transition type (86%) and involved CpG dinucleotides in 50% of the cases. p14^{ARF} and p16^{INK4a} promoter methylation accounted for 80% and 67% of the cases, respectively.

MATERIAL AND METHODS

Patients and samples

Twenty-eight patients suffering from an intestinal-type adenocarcinoma (ITAC) of the nasal cavity and paranasal sinuses untreated previously, operated on at the National Cancer Institute of Milan from 1988–98, were retrieved from the institutional database. Seven patients were excluded since the relative samples were unsuitable for molecular analysis being Boulin-fixed. Twenty-one patients were entered into the study. All but 1 patient (Case 8) was male and presented a disease onset mean age of 61 years (range: 43–79 years) (Table I). Clinical stages included T1, T2, T3 and T4 in 4, 1, 6 and 10 cases, respectively (Table I). Ten patients experienced a professional exposure to wood dust; 4 to leather dust; 1 to marble dust; 1 to carbon monoxide (CO) and particulates and 1 to asbestos (Table III). Three patients showed a non-specific exposure (Cases 8, 17, 21) being a housewife, a nurse and a trader, respectively. For Case 14 no exposure was identified (Table III).

According to the updated AFIP classification,²⁹ the tumors analyzed encompassed 13 moderately differentiated papillary-tubular cylinder cell (PTCC, II), 4 alveolar-goblet cell (AGE), 3 mixed PTCC II+AGE, and 1 signet-ring cell (SRC) carcinomas (Table I).

Microdissection and DNA extraction

Methylene-blue stained sections from formalin-fixed, paraffin-embedded tissues were subjected to a careful microdissection under the microscope to obtain malignant and normal tissues with minimal reciprocal contamination. In 17 cases normal tissue was used as a source of DNA control for microsatellite analysis. Genomic DNA extraction was carried out as described previously.³⁰

H-ras sequencing

PCR reaction was carried out with 200 ng of genomic DNA in 100 µl of a mixture containing 50 µM of each dNTP, 0.2 µM of each primer, 0.75 mM MgCl₂, 1× PCR buffer (Bio Nova, Cambridge, UK) and 1.5 U of KlenTaq1 polymerase (Bio Nova). Primer sequence for H-ras exons 1 and 2 PCR analysis have been described previously.²⁸ PCR conditions: denaturation temperature of 97.5°C (30 sec), annealing of 58°C and 56°C (35 sec) for exon 1

and 2 respectively and elongation of 72°C (55 sec). PCR amplified exons were subjected to automated DNA sequencing (ABIprism 377, Applied Biosystems, Foster City, CA). Each sequencing reaction was carried out at least twice from separate reactions. Results obtained were confirmed on both sense and antisense strands.

Immunocytochemistry

The antibodies applied for immunophenotyping study of p53 and mdm2 proteins were a monoclonal antibody (MAb) to p53 diluted 1:1,000 (DO7; Novocastra, Newcastle upon Tyne, UK) and a MAb to mdm2 diluted 1:1000 (IF2; Oncogene Science, Cambridge, MA). Immunocytochemistry was carried out by the peroxidase-streptavidin method and antigen retrieval was applied as described previously.³⁰

Microsatellite analysis

We studied the incidence of LOH or MSI into and near to the TP53 gene in ITAC by using of 2 markers: p53, a (CA)_n repeat located at chromosome 17p13³⁰ and p53-II, a (AAAAT)_n repeat that mapped into intron 1 of TP53 gene.³¹ We selected 3 microsatellite markers mapped at chromosome 9p21: 1 mononucleotide repeat located into intron 1 of p16^{INK4a} gene (hMp16α-II)³² and 2 dinucleotide repeat markers: D9S942 and IFNA of which sequence was obtained from the Genome Data Base. Two hundred nanograms of genomic DNA were used as template in each PCR reaction in a final volume of 25 µl with the same conditions described in H-ras sequencing. For markers D9S942, hMp16α-II and p53-II we carried out a radiolabeled PCR as described previously.³³ For the other 2 markers we carried out a fluorochrome PCR (5' ABI-Hex IFNA and p53).³⁰ LOH and MSI were defined as described previously.³⁰

DG-DGGE and TP53 sequencing

All samples were screened by DG-DGGE (double gradient-denaturing gradient gel electrophoresis) analysis for the presence of TP53 mutations in the most frequently affected exons (5–8) of the gene. The analysis was carried out in a 2-step PCR protocol. The first amplification step used 50–100 ng genomic DNA in a 25µl reaction volume containing 50 mM KCl, 10 mM Tris-HCl (pH 8.4), 1.5 mM MgCl₂ buffer (Roche, Branchburg, NJ), 80 µM of each dNTP, 0.4 µM final concentration of each primer and 0.65 U of AmpliTaq polymerase (Roche). The PCR profile: 3 min at 95°C; 35 cycles of 15 sec at 95°C, 15 sec at specific annealing temperature, 1 min at 72°C, finally 5 min at 72°C.³⁴ One µl of the diluted amplification product was used as DNA template for the second amplification step. During this PCR step a 40 bp GC-rich sequence (GC-clamp) was attached to the fragments at 5'-end.³⁵ The reaction buffer and cycling conditions were identical to those described above except for an additional final cycle of 5 min at 95°C and 1 hr at 56°C. Primer sequences for the second step of DG-DGGE PCR analysis have been described previously^{35–37} (Table II). The final products of each PCR were electrophoresed on a 3% agarose gel to verify amplification.

DG-DGGE was carried out as described by Gelfi *et al.*³⁸ The denaturant gradient slope was determined according to the melting profile of DNA fragments calculated by utilizing the Macmelt program (Bio-Rad, Hercules, CA). Gels containing a denaturant gradient (40–80%) and a porosity gradient (6.5–12%) were run at 4 V/cm for 16 hr in 1× Tris-acetate/EDTA (TAE) buffer kept at a constant temperature of 60°C. Two types of control for loading were used: a cell line carrying a wild-type TP53 and samples with well-known mutations. After electrophoresis the gels were stained with ethidium bromide. Samples with mutations were identified by the presence for 1 or more new bands or a shift in position compared to the control wild-type cell line and control mutated samples. These cases were subjected to automated DNA sequencing (ABIprism 377, Applied Biosystems) and each sequence reaction was carried out at least twice, analyzing separate amplifications as described previously.³⁹ In each case, the detected

TABLE I – CLINICAL DATA

Case	Age/gender ¹	Histotype ²	UICC stage
1	58/m	PTCC II	T4
2	56/m	PTCC II	T1
3	75/m	PTCC II	T1
4	67/m	PTCC II	T4
5	63/m	AGE	T4
6	67/m	PTCC II	T3
7	53/m	PTCC II	T3
8	46/f	AGE	T3
9	62/m	PTCC II + AGE	T4
10	50/m	PTCC II	T4
11	55/m	AGE	T3
12	51/m	PTCC II	T4
13	43/m	PTCC II	T2
14	78/m	PTCC II + AGE	T4
15	79/m	AGE	T3
16	63/m	PTCC II	T1
17	49/m	PTCC II	T1
18	63/m	PTCC II	T4
19	64/m	SRC	T4
20	58/m	PTCC II + AGE	T4
21	77/m	PTCC II	T3

¹m, male; f, female. ²PTCC, papillary-tubular cylinder cell; AGE, alveolar-globet cell; SRC, signet-ring cell.

TABLE II – PRIMER SEQUENCES AND CONDITIONS OF DG-DGGE

Exon	Primer sequences	Size (bp) ¹	Annealing temperature (degrees)	DGGE condition (% gradient)
5a	5'-GC clamp TTCCTCTTCTACAGTACTC-3' 5'-CGGCACCCGCGTCCGCGCA-3'	158	56	40–70
5b	5'-GC clamp TTCCACACCCCGCCCGCA-3' 5'-TTGCCAGGGTCCCCAG-3'	208	56	50–80
6	5'-GC clamp GAGACGACAGGGCTGGTT-3' 5'-AAGGGTGGTTGTCAGTGG-3'	270	64	40–70
7	5'-GC clamp CAAGGCGCACTGGC-3' 5'-CACTTGCCACCCTGCACACTG-3'	222	64	40–70
8	5'-GC clamp TTCCTTACTGCCTCTTGCTT-3' 5'-GTTATGCCTCAGATTCACTT-3'	271	62	40–75
Sequence of the GC-clamp	5'-CGCCCCGCGCCCCGCGCCCGTCCCGCCGCCCCCGCCCC-3'			

¹Size including the 40-bp GC-clamp.

mutation was confirmed in the sequence as sense and antisense strands.

Homozygous deletion of p14^{ARF} and p16^{INK4a}

Homozygous deletion assay was carried out by a comparative multiplex PCR as described previously.³⁰ The primers used to amplify a 160 bp fragment of p14^{ARF} exon 1β were published by Kourea *et al.*⁴⁰ For the *INK4a* locus the following primers were used: exon 1α, 1108R⁴¹ and p16F (5'-ACG AGG CAG CAT GGA GCC-3'); exon 2, 346R-305F,⁴² 2A (5'-CTG GCT CTG ACC ATT CTG T-3') and F (5'-CAA TTC TCA GAT CAT CAG TCC T-3'); exon 3, X3.90F,⁴² 3C (5'-GCA GTT GTG GCC CTG TAG GA-3'). β-globin gene primers used were: KM38, GH20, PCO4, KM29.⁴³

Analysis of p14^{ARF} and p16^{INK4a} promoter methylation status

DNA methylation patterns in the CpG islands of the p14^{ARF} and p16^{INK4a} genes were determined by methylation-specific PCR (MSP). Bisulfite modification of DNA (2 μg) was carried out as described by Herman *et al.*⁴⁴ One microgram of salmon sperm DNA was added as carrier before modification. We carried out a nested PCR. The bisulfite-modified template was subjected to a Stage-I amplification with primers specific for p14^{ARF} (p14-Forward, 5'-AGT TTG TAG TTA AGG GGG TA-3'; p14-Reverse, 5'-ACT CCT CAA TAC ATC AAC A-3') and p16^{INK4a} genes. Taq Gold polymerase (Applied Biosystems) was used in 50 μl PCR reaction and the annealing temperature was 58°C and 60°C for p14^{ARF} and p16^{INK4a} genes, respectively. The Stage-I PCR products were diluted 10-fold and 4 μl was subjected to a Stage-II PCR in which primers specific to methylated or unmethylated templates were used. Primer sequences of p14^{ARF} were published by Esteller *et al.*⁴⁶ and the annealing temperature was 58.5°C and 68°C for the methylated and unmethylated reaction, respectively. Primer sequences of p16^{INK4a} for the methylated and unmethylated reaction were described previously⁴⁴ and the annealing temperature for both reactions was 68°C. Five micrograms of each PCR reaction was loaded into nondenaturing 6% polyacrylamide gels, stained with ethidium bromide and visualized under UV illumination. We used the cell lines LoVo and Raji as positive control for methylation reaction for p14^{ARF} and p16^{INK4a} genes, respectively.

RESULTS

H-ras sequencing

Molecular analysis of the first 2 exons of H-ras gene was carried out successfully in all cases under study with the exception of Cases 11 and 21 (not evaluable for the exon 1). Using specific primers, no mutations were found in the mostly affected codons 12, 13 and 61 of the H-ras gene (Table III). Nevertheless, a high percentage of cases (62%) presented a base change in 1 or both alleles that gave rise to polymorphisms already described by Capon *et al.*⁴⁷ The H-ras polymorphism frequency of ITAC is

similar to the one of the healthy population. In detail, 12 of 19 (63%) ITACs revealed a H-ras polymorphism at exon 1, codon 27⁴⁸ and 1 ITAC (5%) showed a polymorphism at exon 2, codon 53 (Case 11) (Table III). In addition, Cases 14 and 17 presented a base change at the first intron of the gene (Table III).

Immunocytochemistry

Cumulatively p53 immunoreactivity was observed in 11 of 21 (52%) cases (Table III). Considering the cases with known occupational exposure, 10 of 17 (59%) showed p53 immunoreactivity. A strong immunodecoration involved over 90% of the nuclei in 5 cases (Cases 5, 6, 15, 16 and 21) (Fig. 1a,c) and ranged from 50–80% in the remaining (Fig. 1b) (average 78%). The percentage of nuclear immunostaining in each case is detailed in Table III. No case showed mdm 2 overexpression (Table III).

Microsatellite analysis

The microsatellite analysis at the 9p21 and 17p13 loci through 5 polymorphic markers turned out to be suitable in 16 of 21 ITACs. Overall LOH and MSI were found in 12 of 16 (75%) and 3 of 16 (19%) informative cases, respectively. Considering the ITAC related to a professional exposure we observed LOH in 83% (10 of 12) of the cases. The microsatellite analysis at the locus 9p21 resulted suitable in 15 of 21 cases and overall accounted for 33% of the cases (Table III). All ITACs involved were associated to a professional exposure (5 of 11 = 45%). In Case 2 the LOH occurred at the marker hMp16α-II located into intron 1 of p16^{INK4a} gene. The microsatellite analysis at the 17p13 locus through 2 polymorphic markers turned out to be suitable in 14 of 21 ITACs. Nine of 14 (64%) informative cases revealed LOH in at least 1 of the 2 analyzed microsatellites (Table III). Among the cases related to a professional exposure, 7 (6 to wood dust; 1 to leather dust) of 12 (58%) showed LOH at 17p13 locus (Fig. 2b). In Cases 6, 12, 13 and 14 the LOH occurred at the marker p53-II located into intron 1 of TP53 gene.

Immunocytochemistry correlation

LOH at the locus 17p13 coupled with p53 immunoreactivity was present in 6 of 9 (67%) informative cases. The percentage of nuclear immunostaining intensity and number of involved nuclei ranged from 50–90% (average 77%).

TP53 mutational analysis

TP53 mutational analysis at exons 5–8 was successfully carried out in 20 of 21 cases. PCR-amplified fragments with a different DG-DGGE migration compared to the wild-type control were subjected to automated DNA sequencing. We identified 2 of 20 (10%) cases (Cases 2 and 15) carrying a TP53 polymorphism at exon 6, codon 213,⁴⁹ which does not result in a change in the aminoacid sequences. Mutations were observed in 8 of 20 (40%) cases (Table III). Considering only cases with known professional exposure, however, mutations were observed in 7 of 16 (44%)

TABLE III – TP53, P14^{ARF}, P16^{INK4A} AND H-RAS GENE IMMUNOPHENOTYPING AND GENOTYPING DATA¹

Case	Professional exposure	H-ras mutation	p53/TP53										p16 ^{INK4a} -p14 ^{ARF}						
			ICC		TP53 mutation	17p13 locus		9p21 locus			Homozygos deletion				MSP				
			mdm2	DO7 %		p53	p53-11	D9S942	hMp16α-11	IFNA	ex1β	ex1α	ex2	ex3	P16	P14			
1	Leather dust	WT polym ex1	—	70%	WT	LOH	Neg	Neg	NI	Neg	N	N	N	N	M	M			
2	Wood dust	WT	—	Neg	Polym ex6, Arg213Arg CGA > CGG	Neg	Neg	Neg	LOH	Neg	N	N	N	N	U	M			
3	Wood dust	WT polym ex1	—	50%	WT	LOH	MSI	NI	NI	LOH	N	N	N	N	M	NE			
4	Leather dust	WT polym ex1	—	80%	Mut ex7, Arg248Gln CGG > CAG	Neg	Neg	NI	NI	NI	NE	N	N	N	M	U			
5	Marble dust	WT polym ex1	—	90%	WT	NE	Neg	Neg	NI	LOH	NE	NE	N	N	M	NE			
6	Wood dust	WT polym ex1	—	90%	NE	NI	LOH	Neg	Neg	Neg	NE	NE	NE	N	U	NE			
7	Asbestos	WT polym ex1	—	Neg	Mut ex8, Arg306stop CGA > TGA						N	NE	N	N	M	M			
8	Aspecific	WT	—	Neg	sMut ex5, Val172Val GTT > GTC	NI	NE	Neg	NE	NI	NE	NE	N	N	NE	U			
9	Wood dust	WT	—	Neg	Mut ex6, Arg213stop CGA > TGA						N	N	N	N	M	M			
10	Wood dust	WT	—	70%	Mut ex7, Gly245Asp GGC > GAC	NI	Neg	MSI	NI	Neg	N	N	N	N	M	NE			
11	Leather dust	WT polym ex2	—	Neg	WT	NE	NE	NE	NE	NE	NE	NE	NE	NE	NE				
12	Wood dust	WT polym ex1	—	70%	WT	LOH	LOH	Neg	Neg	NI	NE	NE	N	N	NE	U			
13	Wood dust	WT	—	Neg	Mut ex8, Cys277stop TGT > TGA	NI	LOH	Neg	Neg	LOH	N	N	N	N	U	M			
14	Unknown	WT polym ex1 [^]	—	Neg	WT	LOH	LOH	MSI	NI	Neg	NE	NE	N	N	NE	NE			
15	Leather dust	WT polym ex1	—	90%	Polym ex6, Arg213Arg CGA > CGG						N	N	N	N	M	M			
16	Wood dust	WT	—	90%	Mutex6, Val216Met GTG > ATG	LOH	Neg	Neg	NI	Neg	N	N	N	N	M	M			
17	Aspecific	WT polym ex1 [^]	—	Neg	WT	NI	Neg	Neg	NI	Neg	N	NE	N	N	M	U			
18	Wood dust	WT polym ex1	—	Neg	WT	LOH	Neg	Neg	NI	NI	N	N	N	N	M	M			
19	CO particulates	WT	—	70%	Mut ex7, Arg249Gly AGG > GGG	NI	NE	LOH	NI	Neg	N	N	N	N	U	NE			
20	Wood dust	WT polym ex1	—	Neg	WT						NE	N	NE	NE	U	NE			
21	Aspecific	WT	—	90%	WT	LOH	Neg	Neg	NI	Neg	NE	NE	N	N	NE	NE			
			13/21	62%	11/21	52%	8/20	40%	9/14	64%	5/15	33%				11/16	69%	8/12	67%

¹polym, polymorphism; wt, wild-type; polym ex1, His27His CAT > CAC; polym ex2, Leu53Leu TTG > TTA; [^], base change intron 1, G > A; Mut, mutation; sMut, silent mutation; ex, exon; Pos, positive; Neg, negative; MSI, microsatellite instability; LOH, loss of heterozygosity; NE, not evaluable; NI, non informative; N, normal; M, methylated; U, unmethylated.

TP53, p14^{ARF} AND p16^{INK4a} DEREGULATION IN ITAC

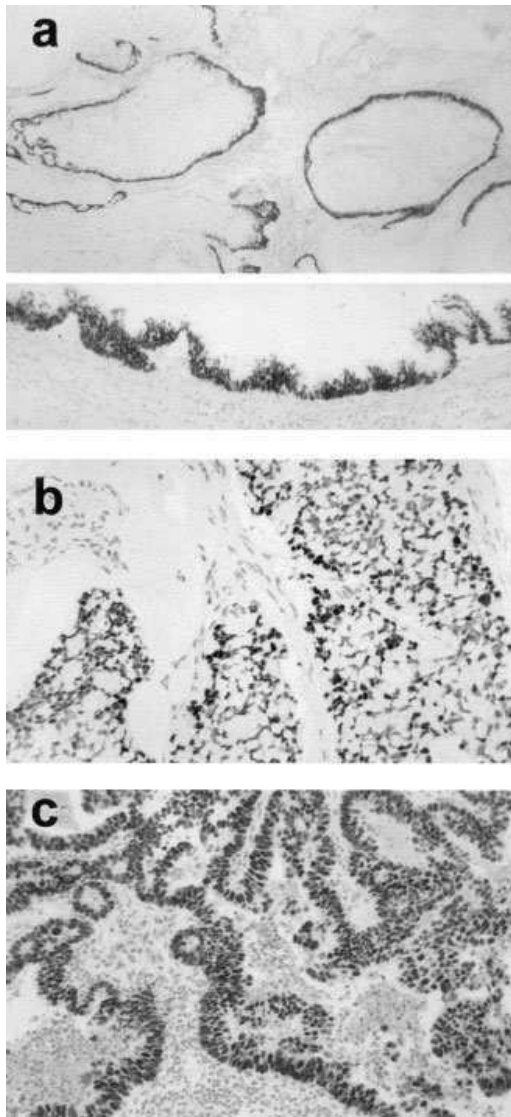


FIGURE 1 – p53 immunophenotype. Strong p53 immunoreactivity in almost all the nuclei in: (a) low power magnification and inset of a case of AGE (Case 15); (b) a case of SRC (Case 19); and (c) a case of PTCC (Case 21) with molecular level evidence of wild-type TP53 carrying polymorphism, missense TP53 mutation, and wild-type TP53, respectively.

cases. One mutation was located in exon 5, 2 in exon 6, 3 in exon 7 and 2 in exon 8. Missense mutations causing an aminoacid substitution were 4 (Cases 4, 10, 16 and 19) and occurred in TP53 mutational hot spots codons (codons 248, 245, 216 and 249, respectively);¹² 1 was a silent mutation in exon 5 codon 172 (Case 8) and the remaining 3 mutated ITACs (Cases 7, 9 and 13) (Fig. 2a) carried a nonsense mutation that leads to the appearance of a premature stop codon and results in an early chain termination during translation (Table III). Except the transversion found in Case 13, all mutations were of the transition type and cumulatively the transitions were 7 of 8 (87%), but accounted for 6 of 7 (86%) if only exposed cases were considered. Three of 7 (43%) and 3 of 6 (50%) transition mutations occurred at CpG dinucleotides in all and exposed cases, respectively.

On the basis of a strong (over 90%) and diffuse p53 immunostaining throughout the tumor, the molecular analysis in Cases 5

and 21 was extended to exons 9 and 10 without finding any alteration. In Case 15 the analysis of exons 9 and 10 was not possible owing to the exiguity of the material.

Immunocytochemistry correlation

The expression of p53 protein well correlated with TP53 mutation analysis. In all cases carrying missense mutations, a positive p53 immunophenotype was observed and, by contrast, a p53 null immunophenotype was detected in all cases with nonsense mutations and in the case with a silent mutation (Table III).

LOH correlation

LOH at the loci 17p13 and 9p21 was found in 2 of 4 (50%) and 2 of 5 (40%) TP53 mutated cases, respectively. The remaining TP53 mutated ITACs were not evaluable or not informative for microsatellite analysis. The percentage of TP53 mutations or LOH at the 17p13 locus was 71%.

Homozygous deletion of p14^{ARF} and p16^{INK4a}

Homozygous deletion analysis was successfully carried out in 20 of 21 ITACs (Case 11 was not evaluable for any exon). No homozygous deletion occurred in any p14^{ARF} and p16^{INK4a} exons (Table III).

MSP

Overall methylation of p14^{ARF} or p16^{INK4a} promoters was detected in 13 of 18 (72%) cases and, considering the exposed ITACs, in 12 of 16 (75%) cases (Fig. 3). Overall p14^{ARF} promoter methylation was observed in 8 of 12 (67%) cases (Table III) and only the cases with known occupational exposure were considered in 8 of 10 (80%). Overall p16^{INK4a} promoter methylation was found in 11 of 16 (69%) cases (Table III). In cases with known occupational exposure, 10 of 15 (67%) showed p16^{INK4a} promoter methylation. Concomitant p14^{ARF} and p16^{INK4a} promoter methylation was present in Cases 1, 7, 9, 15, 16 and 18.

Evidence of TP53 or p14^{ARF} gene deregulation

Overall this accounted for 86% of the cases (18 of 21) and consisted of 8 mutations, 3 of which also carrying LOH at the loci 17p13 or 9p21 and 4 cases also showing p14^{ARF} methylation; 3 LOH at the marker p53-I1 located into intron 1 of TP53 gene associated with a p53 positive immunophenotype in 2 cases; 4 p14^{ARF} promoter methylation coupled with p53 stabilization or LOH at the locus 17p13 (marker p53) in 3 cases; and 3 p53 overexpressing cases, 2 of which with over 90% of the immunostained nuclei, all associated to LOH at the 17p13 or 9p21 loci. Considering only the cases with known occupational exposure, a TP53 or p14^{ARF} gene deregulation was present in 15 of 17 (88%) cases.

Cumulative evidence of p16^{INK4a} alterations

Overall evidence of p16^{INK4a} alterations was found in 60% of cases (12 of 20) and consisted of 11 p16^{INK4a} promoter methylation (2 were also carrying a LOH at the locus 9p21 [marker IFNA]) and 1 LOH at the marker hMp16α-I1 located into intron 1 of p16^{INK4a} gene. Considering only cases with known occupational exposure, the cumulative evidence of p16^{INK4a} alterations accounted for 65% (11 of 17).

Cumulative evidence of TP53 or p14^{ARF} and p16^{INK4a} alterations

Results indicate an alteration of TP53 or p14^{ARF} and p16^{INK4a} genes in 11 of 20 (55%) cases. All ITACs showing concomitant deregulation of these tumor suppressor genes were related to a professional exposure (11 of 16 = 69%).

DISCUSSION

H-ras mutations and the TP53, p14^{ARF} and p16^{INK4a} gene deregulation were investigated in 21 consecutive, untreated cases of ITAC suitable for molecular analyses. The series, in keeping

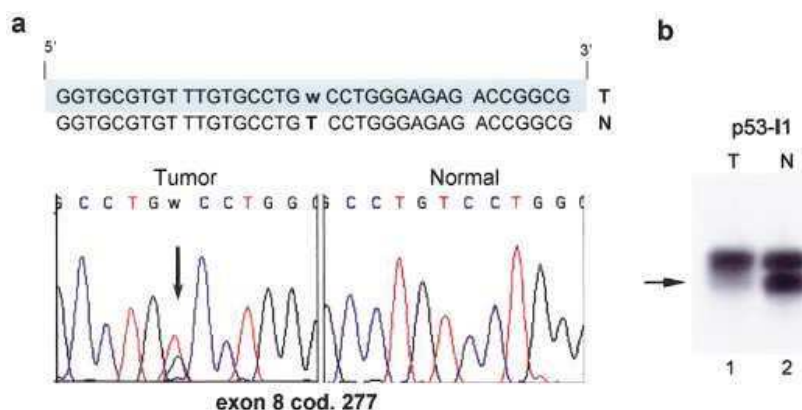


FIGURE 2 – Molecular analysis of a null p53 PTCC case (Case 13) harboring a stop codon TP53 mutation coupled with LOH at locus p53-11. (a) Nucleotide sequence analysis of a portion of the TP53 exon 8 from the tumor DNA showing a Cys277stop, is compared to the sequence from normal DNA control. T, tumor; N, normal tissue. (b) Microsatellite analysis showing a loss of the lower allele (arrow) of the p53-11 polymorphic marker in the tumor (lane 1). The normal tissue (lane 2) shows both alleles. T, tumor; N, normal tissue.

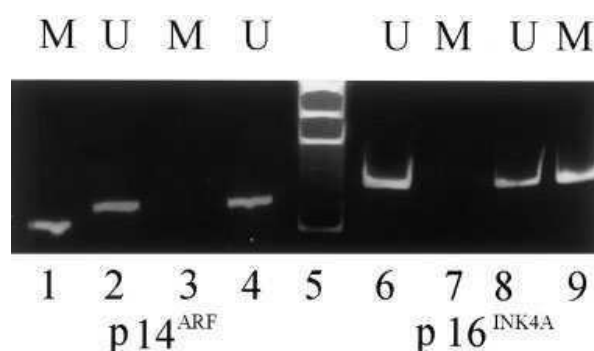


FIGURE 3 – MSP of p14^{ARF} promoter in Cases 1 (lanes 1,2) and 4 (lanes 3,4), and MSP of p16^{INK4a} promoter in Cases 19 (lanes 6-7) and 18 (lanes 8,9). A visible PCR product in lanes marked U and M indicates the presence of unmethylated and methylated promoters, respectively. Molecular weight marker used was ϕ X174 DNA-Hae III digest (lane 5).

with previous epidemiological studies,^{4,5} was found to be associated strongly with male gender, (95%), professional exposure, (85%), as well as prolonged professional exposure. Assuming as reasonable exposure to occupational carcinogens a period exceeding 20 years and a latency period ranging between 0–40 years,²⁸ the mean age of disease onset in our series was 61 years.

The mutations of H-ras gene reported by Perez *et al.*²⁸ in ITAC prompted us to verify this occurrence in our cases. The association between ITAC and environmental mutagens along with the demonstration that chemical carcinogens may cause mutations in the ras gene were in fact both consistent with a possible involvement of ras family genes. In our research, however, codons 12 and 61 of H-ras gene were never found affected by mutations. We cannot rule out that this discrepancy might be ascribed to differences in the genetic background of the target population.

By contrast, we found a high percentage of TP53 mutations or LOH at the 17p13 locus (71%) as well as p53 overexpression (52%) emphasizing the involvement of this tumor suppressor gene in ITAC. TP53 mutations accounted for 8 of 20 cases (40%), and were coupled with LOH at the locus 17p13 in 2 cases. Considering the type of exposure, mutations were found in 7 of 16 (44%) patients exposed to wood/leather/asbestos dusts and in 1 of 3 patients without specific exposure. Interestingly, the latter case carried a silent mutation. In patients with known exposure, all but 1 TP53 mutations, *i.e.*, 6 of 7 (86%), were transitions G:C→A:T, a type of mutation typically related to carcinogen exposure¹² and already reported in 2 cases of ITAC with unknown exposure history.²⁶ The high proportion of this type of mutation strongly suggests a causal relationship between the presence of genotoxic

agents, shared by the various professional dusts, and p53 loss of function. Moreover, 3 of 6 transitions (50%) were at CpG dinucleotide, mutational hot spots that are involved in different types of human cancer¹⁷ being cytosine a target for chemical mutagens inducing enzymatic methylation and guanine a target for a variety of carcinogens.^{15,16} Our results seem to support the idea that CpG sites represent a preferred target of the dust carcinogens and that the properties of carcinogen agents to generate specific type of base substitutions may be influenced by the specific nucleotides sequence.^{13,14,50,51}

The percentage of LOH at the 17p13 locus accounted for 58% in ITACs with known exposure. This type of LOH occurrence seems quite peculiar for ITAC and showed that in a similar percentage of TP53 mutations (43%), LOH at the 17p13 locus reached only 15% (2 of 13)³⁰ in a series of sporadic malignant peripheral nerve sheath tumors that we examined recently. A high rate of LOH at this locus is reported in tumors strongly related to carcinogen exposure such as tobacco smoke-associated larynx cancer²⁰ and in particular, colorectal adenocarcinomas (75%).^{52,53}

In favor of a TP53 deregulation is the uncommon marked and diffuse p53 overexpression found in 10 exposed ITACs (59%) that, besides the 4 TP53 mutated cases, was coupled with LOH at the 17p13 locus in 4 cases. For the remaining 2 cases, where the null mdm2 immunophenotype did not support a p53-mdm2 complex related stabilization,³⁹ we can not rule out the presence of an aberrant mdm2 protein unable to target a correct ubiquitination, but still able to bind a wt p53.⁵⁴

Methylation of p14^{ARF} promoter was found in 80% of ITACs with known professional exposure and this aberration paralleled TP53 mutation in 50% of the cases analyzed (4 of 8). This apparent redundant suppressor gene pathway inactivation is likely to be related to the presence of CpG islands, known to be preferred targets of the dust carcinogens in both p14^{ARF} promoter and TP53 gene.

Regarding p16^{INK4a}, the present results demonstrate a relevant involvement of this tumor suppressor gene in ITACs with known exposure (65%), mainly achieved through an aberrant methylation (67%). The high occurrence of methylation of p14^{ARF} and p16^{INK4a} promoters further underlines the close correlation between dust related genotoxic agents and CpG dinucleotides changes.^{18,19}

p14^{ARF} silencing by promoter methylation is assumed to play a deregulating role into TP53 pathway because the lack of p14^{ARF}-mdm2 binding may negatively affect the p53 function.⁵⁵ Interestingly, TP53 or p14^{ARF} alteration was present in all dust-exposed tumors carrying p16^{INK4a} alterations (69%), suggesting that simultaneous deregulation of these tumors suppressor genes are important in ITAC tumorigenesis.

Moreover, the TP53 and p16^{INK4a} alteration patterns we observed were similar to that reported in colorectal tumors, where the

majority of the *TP53* mutations are G:C→A:T transitions and involve the CpG dinucleotides (54%),^{23,24} and the most of *p16^{INK4a}* alterations are methylation (55%).²⁵ This implies that the morphologic resemblance of ITAC with colorectal adenocarcinoma parallels a similar *TP53* and *p16^{INK4a}* molecular deregulation in contrast to previous observations.²⁶ As for *p14^{ARF}* we found a greater aberrant methylation in our exposed ITACs (80%) compared to that reported in colon carcinomas (28–32%).⁵⁶ *TP53* or *p16^{INK4a}* alterations occur frequently in other lesions of the digestive tract, however, such as the rare small bowel adenocarcinomas⁵⁷ and Barrett's esophagus.^{21,22}

In conclusion, our present study represents the first demonstration, to our knowledge, of *TP53*, *p14^{ARF}* and *p16^{INK4a}* deregulation in ITAC in a series of patients surgically treated and professionally exposed to dusts of different origin. Our results indicate a high occurrence of *TP53* or *p14^{ARF}* (88%) and *p16^{INK4a}* (65%) gene alterations in these tumors, possibly mediated by dust genotoxic agents through a selective action on CpG dinucleotides.^{15,18,19} This interaction is supported by the *TP53* G:C→A:T transition mutations (86%) and the high occurrence of *p16^{INK4a}* or *p14^{ARF}* methylation (75%). Further arguments in favor of this conclusion are provided by the LOH at chromosomal loci encoding the *TP53*, *p14^{ARF}* and *p16^{INK4a}* genes, a molecular event already reported as being associated closely with carcinogenic exposure.²⁰

Because there is mounting evidence that puts forth the knowledge that both tumor genotype and mechanisms of drug action are determinants for selecting effective treatments using current chemotherapy regimens, our insights may be helpful in planning more tailored treatments. Alterations found in ITAC are likely to carry relevant biological implications given the important role that both *TP53* and *p16^{INK4a}* play in cell growth control and apoptosis. Most of DNA-damaging drug-based regimes applied currently utilize an intact apoptotic pathway that is disabled by *INK4a/TP53* gene alterations making the drug apoptosis-mediated cell killing mechanism ineffective.^{58,9} In our series, this is expected for *TP53* mutation-carrying cases. In *p16^{INK4a}* methylation-carrying cases a complete loss of function of the encoded protein may only be assumed because the MSP approach does not provide information about silencing of both the alleles. We are evaluating gene profile vs. response to therapy in a biopsy-based series of ITACs treated by conventional primary chemotherapy followed by surgery.

ACKNOWLEDGEMENTS

We thank M. Frattini, Ph.D. and D. Balestra, Ph.D. for kindly providing the *p16^{INK4a}* MSP protocol and Mrs. M. Azzini and G. Roncato for photographic assistance.

REFERENCES

- Barnes L. Intestinal-type adenocarcinoma of the nasal cavity and paranasal sinuses. *Am J Surg Pathol* 1986;10:192–202.
- Franquemont DW, Fechner RE, Mills SE. Histologic classification of sinonasal intestinal-type adenocarcinoma. *Am J Surg Pathol* 1991;15:368–8.
- Licitra L, Locati L, Cavina R, Garassino I, Mattavelli F, Pizzi N, Quattrone P, Valagussa P, Cantu' G. Primary chemotherapy (PC), followed by cranio-facial resection (Cfr) and post-operative radiotherapy (Rt), for sinonasal ethmoid cancer (Ec): a pilot study. *Proc Am Soc Clin Oncol* 2000;19:431a.
- Acheson ED, Cowdell RH, Hadfield E, Macbeth RG. Nasal cancer in woodworkers in the furniture industry. *BMJ* 1968;2:587–96.
- Acheson ED, Cowdell RH, Jolles B. Nasal cancer in the Northamptonshire boot and shoe industry. *BMJ* 1970;1:385–93.
- Leclerc A, Martinez Cortes M, Gerin M, Luce D, Brugere J. Sinonasal cancer and wood dust exposure: results from a case-control study. *Am J Epidemiol* 1994;140:340–9.
- Battista G, Comba P, Orsi D, Norpoth K, Maier A. Nasal cancer in leather workers: an occupational disease. *J Cancer Res Clin Oncol* 1995;121:1–6.
- Wolf J, Schmezer P, Fengel D, Schroeder HG, Scheithauer H, Woeste P. The role of combination effects on the etiology of malignant nasal tumours in the wood-working industry. *Acta Otolaryngol Suppl* 1998;535:1–16.
- Luce D, Gerin M, Morcet JF, Leclerc A. Sinonasal cancer and occupational exposure to textile dust. *Am J Ind Med* 1997;32:205–10.
- Leclerc A, Luce D, Demers PA, Boffetta P, Kogevinas M, Belli S, Bolm-Audorff U, Brinton LA, Colin D, Comba P, Gerin M, Hardell L, et al. Sinonasal cancer and occupation. Results from the reanalysis of twelve case-control studies. *Am J Ind Med* 1997;31:153–65.
- Van den Oever R. Occupational exposure to dust and sinonasal cancer. An analysis of 386 cases reported to the N.C.C.S.F. Cancer Registry. *Acta Otorhinolaryngol Belg* 1996;50:19–24.
- Greenblatt MS, Bennett WP, Hollstein M, Harris CC. Mutations in the p53 tumor suppressor gene: clues to cancer etiology and molecular pathogenesis. *Cancer Res* 1994;54:4855–78.
- Khalil H, Zhang FJ, Harvey RG, Dipple A. Mutagenicity of benzo[a]pyrene-deoxyadenosine adducts in a sequence context derived from the p53 gene. *Mutat Res* 2000;465:39–44.
- Loechler EL. The role of adduct site-specific mutagenesis in understanding how carcinogen-DNA adducts cause mutations: perspective, prospects and problems. *Carcinogenesis* 1996;17:895–902.
- Weisenberger D, Romano L. Cytosine methylation in a CpG sequence leads to enhanced reactivity with Benzo[a]pyrene Diol Epoxide that correlates with a conformational change. *J Biol Chem* 1999;274:23948–55.
- Denissenko M, Chen J, Tang M, Pfeifer G. Cytosine methylation determines hot spots of DNA damage in the human P53 gene. *Proc Natl Acad Sci USA* 1997;94:3893–8.
- Hollstein M, Sidransky D, Vogelstein B, Harris CC. p53 mutations in human cancers. *Science* 1991;253:49–53.
- Kim DH, Nelson HH, Wiencke JK, Zheng S, Christiani DC, Wain JC, Mark EJ, Kelsey KT. p16^{INK4a} and histology-specific methylation of CpG Islands by exposure to tobacco smoke in non-small cell lung cancer. *Cancer Res* 2001;61:3419–24.
- Weihrauch M, Benicke M, Lehnert G, Wittekind C, Wrbitzky R, Tannapfel A. Frequent k-ras-2 mutations and p16^{INK4a} methylation in hepatocellular carcinomas in workers exposed to vinyl chloride. *Br J Cancer* 2001;84:982–9.
- Szyfyer K, Szmaja Z, Szyfyer W, Hemminki K, Banaszewski J, Jaskula-Zstul R, Louhelainen J. Molecular and cellular alterations in tobacco smoke-associated larynx cancer. *Mutat Res* 1999;445:259–74.
- Jenkins GJS, Doak SH, Parry JM, D'Souza FR, Griffiths AP, Baxter JN. Genetic pathways involved in the progression of Barrett's metaplasia to adenocarcinoma. *Br J Surg* 2002;89:824–37.
- Wong DJ, Paulson TG, Prevo LJ, Galipeau PC, Longton G, Blount PL, Reid BJ. P16^{INK4a} lesion are common early abnormalities that undergo clonal expansion in Barrett's metaplastic epithelium. *Cancer Res* 2001;61:8284–9.
- Tang R, Pei-Feng W, Wang HC, Wang JY, Hsieh LL. Mutations of p53 gene in human colorectal cancer: distinct frame-shifts among populations. *Int J Cancer* 2001;91:863–8.
- Rodrigues NR, Rowan A, Smith MEF, Kerr IB, Bodmer WF, Gannon JV, Lane DP. p53 mutations in colorectal cancer. *Proc Natl Acad Sci USA* 1990;87:7555–9.
- Guan RJ, Fu Y, Holt PR, Pardee AB. Association of K-ras mutation with p16 methylation in human colon cancer. *Gastroenterology* 1999;116:1063–71.
- Wu TT, Barnes L, Bakker A, Swalsky PA, Finkelstein SD. K-ras-2 and p53 genotyping of intestinal-type adenocarcinoma of the nasal cavity and paranasal sinuses. *Mod Pathol* 1996;9:199–204.
- Saber AT, Nielsen LR, Dictor M, Hagmar L, Mikoczy Z, Wallin H. K-ras mutations in sinonasal adenocarcinomas in patients occupationally exposed to wood or leather dust. *Cancer Lett* 1998;126:59–65.
- Perez P, Dominguez O, Gonzalez S, Gonzalez S, Trivino A, Suarez C. Ras gene mutations in ethmoid sinus adenocarcinoma. *Cancer* 1999;86:255–64.
- Franquemont W, Fechner R, Mills S. Histologic classification of sinonasal intestinal-type adenocarcinoma. *Am J Surg Pathol* 1991;15:368–75.
- Birindelli S, Perrone F, Oggionni M, Lavarino C, Pasini B, Vergani B, Ranzani GN, Pierotti MA, Pilotti S. Rb and TP53 pathway alterations in sporadic and NF1-related malignant peripheral nerve sheath tumors (MPNSTs). *Lab Invest* 2001;81:833–44.
- Yamamoto Y, Kishimoto Y, Wistuba II, Virmani AK, Vuitch F, Gazdar AF, Albores-Saavedra J. DNA analysis at p53 locus in carcinomas arising from pleomorphic adenomas of salivary glands: com-

- parison of molecular study and p53 immunostaining. *Pathol Int* 1998; 48:265–72.
32. Herranz M, Urioste M, Santos J, Rivas C, Martinez B, Benitez J, Fernandez-Piqueras J. Analysis of the INK4a/ARF locus in non-Hodgkin's lymphomas using two new internal microsatellite markers. *Leukemia* 1999;13:808–10.
 33. Birindelli S, Tragni G, Bartoli C, Ranzani GN, Rilke F, Pierotti MA, Pilotti S. Detection of microsatellite alterations in the spectrum of melanocytic nevi in patients with and without individual or family history of melanoma. *Int J Cancer* 2000;86:255–61.
 34. Donghi R, Longoni A, Pilotti S, Michieli P, Della Porta G, Pierotti MA. Gene p53 mutations are restricted to poorly differentiated and undifferentiated carcinoma of the thyroid gland. *J Clin Invest* 1993; 91:1753–60.
 35. Renault B, van den Broek M, Fodde R, Wijnen J, Pellegata N, Amadieu D, Khan PM, Ranzani GN. Base transitions are the most frequent genetic changes at p53 in gastric cancer. *Cancer Res* 1993; 53:2614–7.
 36. Top B, Mooi W, Klaver S, Boerrigter L, Wisman P, Elbers HR, Visser S, Rodenhuis S. Comparative analysis of p53 gene mutations and protein accumulation in human non-small-cell lung cancer. *Int J Cancer* 1995;64:83–91.
 37. Di Giuseppe J, Hruban R, Offerhaus G, Clement H, van de Berg F, Cameron J, van Mansfeld ADM. Detection of K-ras mutations in mucinous pancreatic duct. Hyperplasia from a patient with a family history of pancreatic carcinoma. *Am J Pathol* 1994;44:889–95.
 38. Gelfi C, Righetti S, Zunino F, Della Torre G, Pierotti MA, Rigetti PG. Detection of p53 point mutations by double-gradient denaturing gradient gel electrophoresis. *Electrophoresis* 1997;18:2921–7.
 39. Pilotti S, Della Torre G, Lavarino C, Di Palma S, Sozzi G, Minoletti F, Rao S, Pasquini G, Azzarelli A, Rilke F, Pierotti MA. Distinct mdm2/p53 expression patterns in liposarcoma subgroups: implications for different pathogenetic mechanisms. *J Pathol* 1997;181:14–24.
 40. Kourea HP, Orlow I, Scheithauer BW, Cordon-Cardo C, Woodruff JM. Deletions of the INK4A gene occur in malignant peripheral nerve sheath tumors but not in neurofibromas. *Am J Pathol* 1999;155:1855–60.
 41. Kamb A, Shattuck-Eidens D, Eeles R, Liu Q, Gruis NA, Ding W, Hussey C, Tran T, Miki Y, Weaver-Feldhaus, McClure M, Aitken JF, et al. Analysis of the p16 gene (CDKN2) as a candidate for the chromosome 9p melanoma susceptibility locus. *Nat Genet* 1994;8: 22–6.
 42. Hussussian CJ, Struwing JP, Goldstein AM, Higgins PAT, Ally DS, Sheahan MD, Clark Jr WH, Tucker MA, Dracopoli NC. Germline p16 mutations in familial melanoma. *Nat Genet* 1994;8:15–21.
 43. Lawn RM, Efstratiadis A, O'Connell C, and Maniatis T. The nucleotide sequence of the human β -globin gene. *Cell* 1980;21:647–51.
 44. Herman JG, Graff JR, Myohanen S, Barry Nelkin D, Baylin SB. Methylation-specific PCR: a novel PCR assay for methylation status of CpG islands. *Proc Natl Acad Sci USA* 1996;93:9821–6.
 45. Palmisano WA, Divine KK, Saccomanno G, Gilliland FD, Baylin SB, Herman JG, Belinsky SA. Predicting lung cancer by detecting aberrant promoter methylation in sputum. *Cancer Res* 2000;60:5954–8.
 46. Esteller M, Cordon-Cardon C, Corn PG, Meltzer SJ, Pohar KS, Watkins DN, Capella G, Peinado MA, Matias-Guiu X, Prat J, Baylin SB, Herman JG. p14^{ARF} silencing by promoter hypermethylation mediates abnormal intracellular localization of MDM2. *Cancer Res* 2001;61:2816–21.
 47. Capon DJ, Chen EY, Levinson AD, Seeburg PH, Goeddel DV. Complete nucleotide sequences of the T24 human bladder carcinoma oncogene and its normal homologue. *Nature* 1983;320:33–7.
 48. Hoban PR, Santibanez-Koref MF, Kelsey AM. Polymorphism in exon 1 of the c-Ha-ras gene, (HRAS). *Nucleic Acids Res* 1991;19:6976.
 49. Carbone D, Chiba I, Mitsudomi T. Polymorphism at codon 213 within the p53 gene. *Oncogene* 1991;6:1691–2.
 50. Chen B, Liu L, Castonguay A, Maronpot R, Anderson M, You M. Dose-dependent ras mutation spectra in N-nitrosodimethylamine induced mouse liver tumors and 4-(methylnitrosamino)-1-(3-pyridyl)-1-butanone induced mouse lung tumors. *Carcinogenesis* 1993;14: 1603–8.
 51. Holmquist G, Gao S. Somatic mutation theory, DNA repair rates, and the molecular epidemiology of p53 mutations. *Mutat Res* 1997;386: 69–101.
 52. Baker SJ, Fearon ER, Nigro JM, Hamilton SR, Preisinger AC, Jessup JM, vanTuinen P, Ledbetter DH, Barker DF, Nakamura Y, White R, Vogelstein B. Chromosome 17 deletions and p53 gene mutations in colorectal carcinomas. *Science* 1989;244:217–21.
 53. Baker SJ, Preisinger AC, Jessup JM, Paraskeva C, Markowitz S, Willson JKV, Hamilton S, Vogelstein B. p53 gene mutations occur in combination with 17p allelic deletions as late events in colorectal tumorigenesis. *Cancer Res* 1990;50:7717–22.
 54. Tamborini E, Agus V, Perrone F, Papini D, Romanò R, Pasini B, Gronchi A, Colecchia M, Rosai J, Pierotti MA, Pilotti S. Lack of SYT-SSX fusion transcripts in malignant peripheral nerve sheath tumors on RT-PCR analysis of 34 archival cases. *Lab Invest* 2002; 82:609–18.
 55. Robertson KD, Jones PA. The human ARF cell cycle regulatory gene promoter is a CpG island which can be silenced by DNA methylation and down-regulated by wild-type p53. *Mol Cell Biol* 1998;18:6457–73.
 56. Jubb AM, Bell SM, Quirke P. Methylation and colorectal cancer. *J Pathol* 2001;195:111–34.
 57. Achille A, Baron A, Zamboni G, Orlandini S, Bogina G, Bassi C, Iacono C, Scarpa A. Molecular pathogenesis of sporadic duodenal cancer. *Br J Cancer* 1998;77:760–5.
 58. Schmitt CA, Fridman JS, Yang M, Lee S, Baranov E, Hoffman RM, Lowe SW. A senescence program controlled by p53 and p16^{INK4a} contributes to the outcome of cancer therapy. *Cell* 2002;109:335–46.
 59. Johnstone RW, Ruefli AA, Lowe SW. Apoptosis: a link between cancer genetics and chemotherapy. *Cell* 2002;108:153–64.